Fatigue Strength of Longitudinal Fillet Welded Joints in Hybrid Girders

Résistance à la fatigue des soudures d'angle, dans les poutres hybrides

Dauerfestigkeit der Längskehlnähte bei hybriden Vollwandträgern

T. YAMASAKI
General Manager

M. HARA
Senior Research Engineer

Y. KAWAI
Research Engineer

Steel Structure Research Laboratories, Kawasaki Steel Co., Ltd.
Chiba, Japan

I. Introduction

In this decade several investigations were conducted to study static and fatigue strength of hybrid girders in U.S.A. (1~6) and Japan(7~9), and some of these data were adopted into design specifications for U. S. highway bridges(10) and buildings(11).

On fatigue strength of hybrid girders, Toprac et al. pointed out based on their significant experimental study that there are three distinctive types of fatigue cracks, initiated at different locations and by different causes in hybrid girders under pure bending, as shown in Fig. 1.(5). Regarding Type 3 crack, Specifications for Highway Bridges in U. S. A. (10) specifies that stiffener to web and flange-web fillet weld connection shall be designed for fatigue based on the flange steel.

The purpose of the present work is to explore the data of fatigue strength of Type 3 crack in hybrid girders and to study the crack propagation behavior at tension flanges and webs. Test results obtained by model specimens are discussed on fatigue strength with reference to structural behavior of hybrid plate girders subjected to repeated bending by usual analytical procedures (S-N relations) and fracture mechanics.

II. Test Specimens and Procedures

Test specimens and test procedures were simulated to those proposed by Reemsnyder (13) by using tee-shaped hybrid specimens consisting of WES-HW 70 (heat treated constructional alloy steel with minimum specified tensile strength of $80 \, kg/mm^2$) at simulating flange plates and JIS-SS41(structural carbon steel with minimum specified tensile strength of $41 \, kg/mm^2$) at simulating wed plates, under axial pulsating tension.

Ten axially loaded fillet welded tee-shaped specimens were tested at a stress ratio of R=0.1(≒0) (one of these was a large-sized specimen), and four were at a stress ratio of R=0.5. These specimens were submerged-arc welded with an intermediate strength filler metal-flux combination. The lower strength filler metal-flux combination than flange steel is preferred the fillet welding between constructional alloy steel and mild steel because of its economy and its
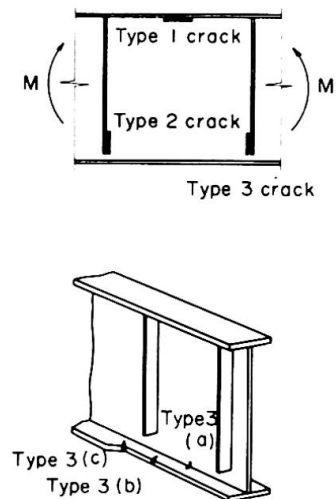

Fig. 1 Types of fatigue cracks under pure bending

ductility (7, 13). No non-destructive inspections, radiography or urtra-sonic inspection were performed before fatigue testing, assuming that the most unfavourable conditions exited. Details of the tee-specimens are shown in Fig. 2, and the mechanical properties and chemical compositions are summarized in Table 1.

All specimens were tested in 150-ton electro-hydraulic alternating testing machine at about 300 c. p. m. and applied stresses during fatigue test were monitored by dynamic strain measurements and a load cell and fatigue crack propagations were measured by using crack gauges when fatigue crack initiations were observed.
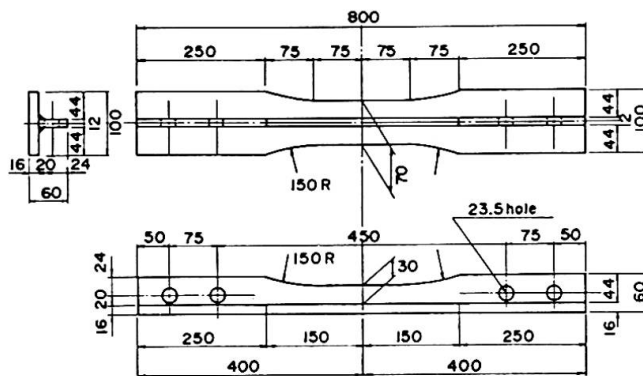

Fig. 2 Details of test specimen

Table 1. Mechanical properties and chemical compositions

	Thickness (mm)	Chemical Compositions (Wt %)												Mechanical Properties			
		C	Si	Mn	P	S	Cu	Ni	Cr	Mo	V	B	Ceq	Y.P. (kg/mm²)	U.T.S. (kg/mm²)	Elong. (%)	vE-e (kg-m)
WES-HW70 (Base Plate)	16	0.100	0.30	0.85	0.007	0.010	0.19	0.78	0.46	0.33	0.035	0.004	0.45	80	84	32	15.6
JIS-SS41 (Rib Plate)	12	0.14	0.033	1.17	0.009	0.021	—	—	—	—	—	—	—	29	47	35	—
Weld Metal (KW-101B)	φ 4	0.06	0.24	1.45	0.013	0.009	—	0.77	—	0.41	—	—	—	57	66	26	—

III. Test Results and Discussion

III — 1 Test Results

The fatigue test results are summarized in Table 2 and are shown graphically in Fig. 3. All the test results are discussed in relation to applied stress range at welds S_r and number of cycles to failure N_f.

Although the test results at different stress ratios of R=0 and R=0.5 are plotted irrespectively, the data fall in a certain scatter band. Judging from this fact, the effect of mean stress may be neglected in these stress ratios of 0 to 0.5. The regression analysis of all the present test results obtained by the method of least squares with reference to the number of cycles to failure and the stress range gives eq. (1).

$$\text{Log } N_f = 11.790 - 4.218 \text{ Log } S_r \quad \cdots\cdots\cdots\cdots\cdots\cdots (1)$$

Table 2. Summary of Test Results

No	TEST PIECE	APPLIED STRESS (kg/mm²)			STRESS RATIO (R.)	FIRST OBSERVATION (x10⁴)	CYCLES TO FAILURE (x10⁴)	CRACK INITIATION MODE[b]
		MAX (Smax)	MIN (Smin)	RANGE (Sr)				
1	T.P- No.1	25.9	2.7	23.2			124.50	N
2	T.P- No.2	28.8	2.8	26.0		88.11	91.65	W
3	T.P- No.3	33.8	3.2	30.6			24.85	26.17	N
4	T.P- No.4	20.8	2.2	18.6			267.21[a]	—
5	T.P- No.5	21.4	2.1	19.3	0.1		228.20	C
6	T.P- No.7	32.4	3.1	29.3			43.00	W
7	T.P- No.8	24.1	2.3	21.8		205.62	212.60	W
8	T.P- No.9	34.3	1.6	32.7		26.23	27.04	W
9	T.P- No.12	23.2	2.3	20.9		91.00	93.92	W
10	T.P- No.6	47.4	24.2	23.2		154.13	158.02	W
11	T.P- No.10	40.4	19.7	20.7	0.5	162.50	166.88	C
12	T.P- No.11	52.2	26.6	25.6			41.91	C
13	T.P- No.13	36.7	18.0	18.7			263.52[a]	—
14	T.P- No.14	19.5	1.7	17.8	0.1		257.00[a]	—

a) No failure

W: Embedded Defect (Wormhole)   C: Under-cut   N: Surface Notch

b) Crack Initiation Mode

Stress Range (kg/mm²)

O R ÷ O
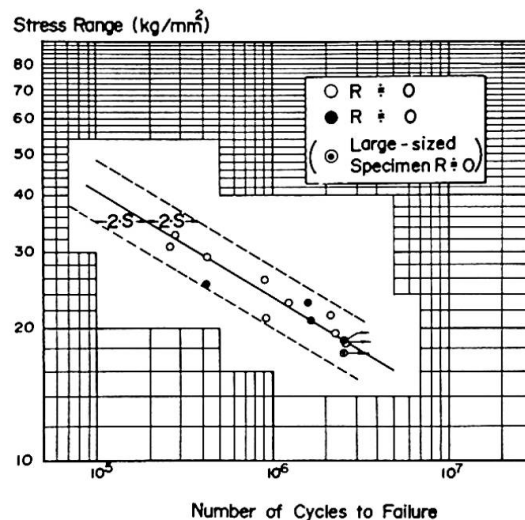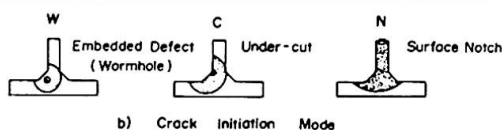● R ÷ O
◉ Large-sized Specimen R ÷ O

Number of Cycles to Failure

Fig. 3 Fatigue test results

The mean regression line is shown in Fig. 3 together with its confidence limits. The fatigue strength at 2×10^6 cycles in stress range are estimated at $20.0 \, kg/mm^2$ (mean) and $16.9 \, kg/mm^2$ (95% confidence limit). The behavior of cyclic specimens was very consistent in spite of the fact that yielding was occurred at web plates in the several specimens subjected to higher maximum stresses.

The observed crack initiation modes were divided into three types and the mode applying to any specimen is recorded in Table 2 and typical fracture surface of three types of crack initiations are shown in Figs. 4 to 6. Among these initiation modes, the most frequent initiatition was type W, and this fact agreed with the fatigue test results of homogeneous beams by Fisher et al. (14).
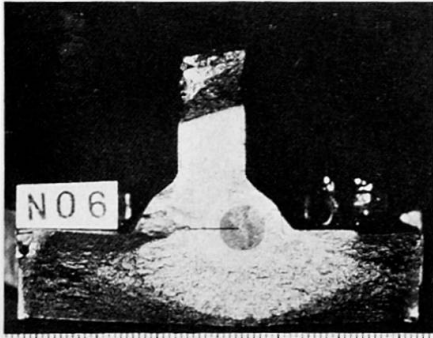

Fig. 4 Fracture surface
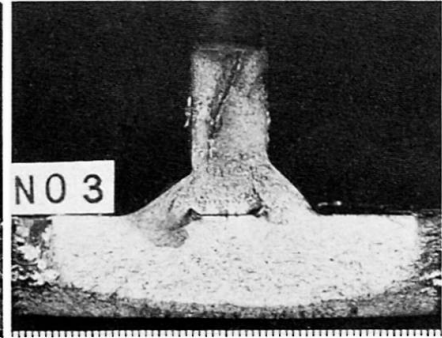(from worm-hole)

Fig. 5 Fracture surface
(from under-cut)

Fig. 6 Fracture surface
(from surface notch)

III—2 Comparisons with Previous Fatigue Data

The fatigue data of hybrid girders can be conventionally compared with those of homogeneous ones (5.6). There are several investigations into the fatigue strength of high strength steel girders and longitudinal fillet welded joints comparable with the present test results. The comparisons between these fatigue strength were extensively discussed in Ref. (15). Fig. 7 shows the additional comparisons with these available fatigue data for analysis of Type 3 crack. In paticular, the work by Reemsnyder (13) on the fatigue strength of longitudinal fillet weld in constructional alloy steel is most comparable, because the present test pieces and test procedure are simulated to those of that work. The two test results shown in Fig. 7, that is, solid circles and the hollow circles represent the test results obtained by using hybrid specimens and homogeneous ones respectively, and they seem to agree well with each other in spite of disregarding the effect of the mean stress. Again, a study of Fig. 7 reveals that the fatigue strength of tee-shaped model specimens and those of beams consisting of $80 \, kg/mm^2$ class high strength steel are not significantly different.

Furthermore, there are two other comparable previous works that are essential. Fig. 8(a) and Fig. 8(b) are quoted from these works dy Frost(4) and Toprac(5), respectively. Both figures represent the comparisons between the test results
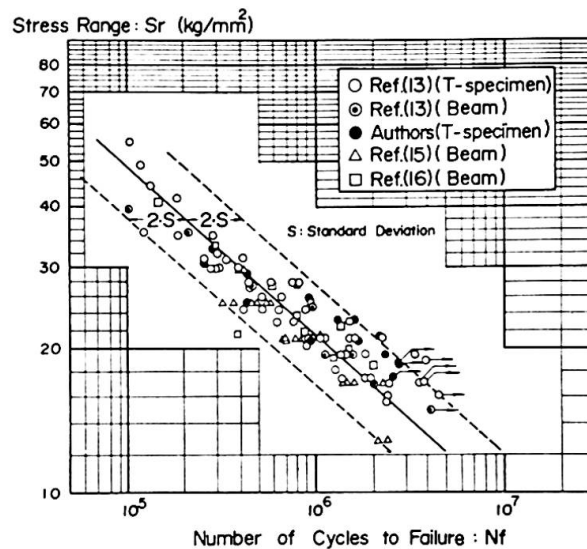

Fig. 7 Comparison of previous work on Type 3 crack with this study

of hybrid girders consisting of 80 kg/mm² class high strength steel in flanges (4,5) and these of tee-shaped homogeneous specimens(13). It seems that the former ones are slight higher than the latter, especially in the case of Fig. 8(b). The disagreement in Fig. 8(b) was concluded by Toprac that such a difference could be attributed to the fact that the tee-shaped specimens were fabricated under a controlled condition, whereas the girder specimens were fabricated with an average commercial shop practice. This conclusion implies that the fatigue strength, especially regarding to Type 3 crack, is largely influenced by welding conditions and fabrication methods.
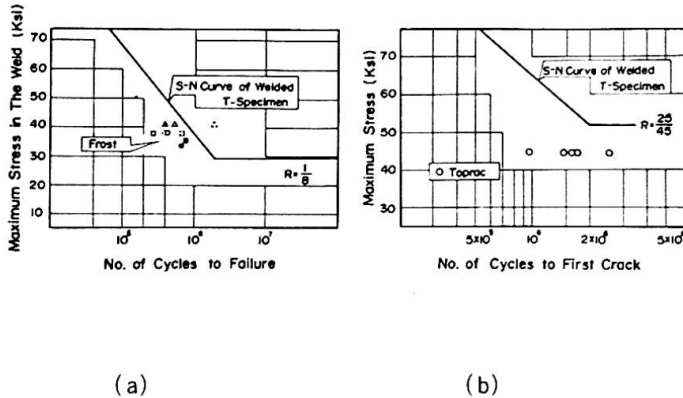

(a)   (b)

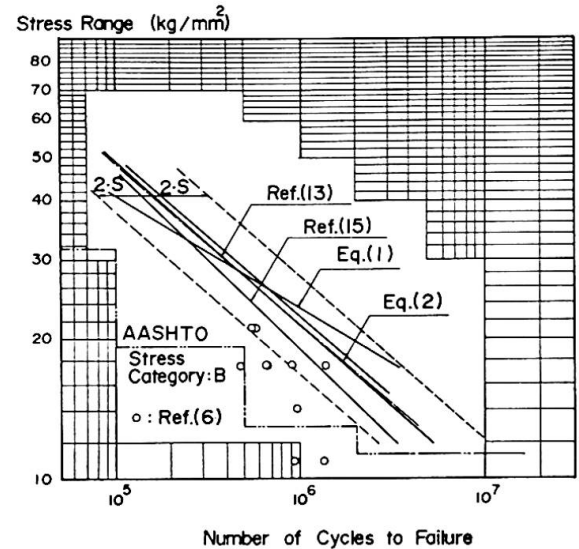Fig. 8 Comparison of fatigue date on hybrid beams with homogeneous tee-shaped specimens

Fig. 9 Comparison of related S-N curves with design stress

The regession analysis of all the available test results by the method of least squares gives

$$\text{Log } N_f = 9.720 - 2.800 \text{ Log } S_r \quad \cdots\cdots\cdots\cdots\cdots (2)$$

and fatigue stregths at 2×10^6 cycles of web-to-flange fillet weleded joints consisting of 80 kg/mm² class high strength steel in flanges are estimated at 16.7 kg/mm² (mean) and 12.9 kg/mm² (95% confidence limit) in stress range. Shown in Fig. 9 is all the available S-N curves related to longitudinal fillet weldments in web-to-flange junctures, using the mean regression lines and the limits of dispersion correspoding to the 95% confidence limits in comparison with fatigue allowable stresses specified in AASHTO Specifications.

It will be resonable, if Toprac's result is ignored, that the clause in AASHTO(10,17) provides that web to flange weld connections in hybrid girders shall be designed for preventing fatigue based on the flange steel and that allowable fatigue stresses are given in terms of stress ranges.

III－3 Fatigue Behavior Prediction by Fracture Mechanics

The relation betwee the fatigue crack-growth rate and the change in the stress intensity factor is presented in the form of

$$da/dN = C(\Delta K)^m \quad \text{(mm/cycle)} \quad \cdots\cdots\cdots\cdots\cdots (3)$$

where a is a half length of fatigue crack and ΔK the variation of the stress intensity factor $(K_{max} - K_{min})$; C and m are material constants. And, the stress intensity factor usually takes the form

$$K = \sigma\sqrt{\pi a} \cdot f(a) \quad \text{(kg/mm}^{-3/2}) \quad \cdots\cdots\cdots\cdots\cdots (4)$$

where σ and f(a) respectively represent remotely applied stress and a correction function to which the dimensions of the plate, the distance to a free edge or surface and the shape of cracks are introduced. From eqs. (3) and (4), the fatigue life N is given as

$$N = \frac{1}{C(\Delta\sigma)^m} \int_{a_i}^{a_f} \frac{da}{a^{m/2} \cdot \pi^{m/2} \cdot f^m(a)} \quad \cdots\cdots\cdots\cdots\cdots (5)$$

where a_i and a_f are the initial and final crack sizes, respectively. On the other hand, the conventional S-N relation is represented as follows

$$\text{Log } N = C' - n \cdot \text{Log}(\Delta\sigma) \quad \cdots\cdots (6)$$

where N and $\Delta\sigma$ are the fatigue lives and the applied stress ranges respectively and C' and n are material constants. Fisher et al.(14) introduced the relationship among these constants, in eqs. (3) and (6) that characterize the fatigue crack growth rate and the S-N curve, respectively, as follows.

$$m = n \qquad (7\text{-}a)$$

and

$$C' = \text{Log}\left[\frac{1}{C} \cdot \frac{(a_i^{-\alpha} - a_f^{-\alpha})}{\alpha \cdot f^m(a) \pi^{m/2}}\right] \quad (7\text{-}b)$$

where, $\alpha = m/2 - 1$.

Fig. 10 Fatigue crack-growth rate

This relationship is based on an approximate assumption as the correction function f(a) does not vary under constant amplitude stress.

The relationship among the material constants represented in the form of eq.(7) is obtained for homogeneous beams where the crack growth rate is isotropic. All the previous works conducted on fatigue crack growth rates dealt with almost homogeneous materials. Accordingly, it was questionable whether such relation could be applied to hybrid members consisting of different steel grades, since Gurney (19) indicated the relation of m and Log C to be linear functions of yield stress of the material. The fracture surfaces observed in the present test, however, suggest the possibility of the application of the above relation, because it is recognized that the fatigue fracture surfaces indicate concentric circles as is typically shown in Fig. 8 and the fatigue crack growth rate may be isotropic.

Fisher et al. (14) also made an assumption to evaluate the crack growth constants, C and m, that the porosity was assumed to be described by a disc-like penny-shaped crack with a constant correction factor, f(a), over the interval of integration of $2/\pi$.

In the present work, the initial crack radius, a_i, for the evaluation of the crack-growth constants, C and m, was assumed 0.5mm that is the mesured tip radius of elongated worm-holes. The final crack radius, a_f, was assumed to be the flange thickness, The equation of the mean regression line from the method of least squares applied to the test data for specimens failing from embedded weld defects in the longitudinal fillet weld is

$$\text{Log } N_f = 11.388 - 3.895 \text{ Log } S_r \quad \cdots\cdots\cdots (8)$$

Thus, the material constants corresponding to C' and n in eq.(6) are 2.443×10^{11} and 3.895. From the above mentioned assumptions and eq.(7), the crack-growth constants, C and m, are evaluated and the fatigue crack growth-rate are represented numerically as

$$da/dN = 5.0 \times 10^{-12} \times (\Delta K)^{3.9} \quad \cdots\cdots\cdots (9)$$

Eq. (9) as described from the mean regression curve of fatigue test data is shown in Fig. 10 and compared with the data points for the measured crack-growth rates on inside surface of the flange for growth as a three-ended crack. The data points are compared well with the estimated curve up to the ΔK of about 100kg/mm$^{-3/2}$ where crack penetrates the extreme fiber of flanges. The derived crack-growth relationship given by Fisher et al.(14) and a conservative upper bound for growth-rates on ferrite-pearlite steels proposed by Barsom (18) are also compared with the present test results. These works gave the m-value of 3 and the one obtained by the present test was about 4 that is the preliminary proposed value by Paris (21). Kitagawa et al. (20) found a convenient correlation between C and m for a number of data obtained by different investigators. The correlation curve is expressed in the form of
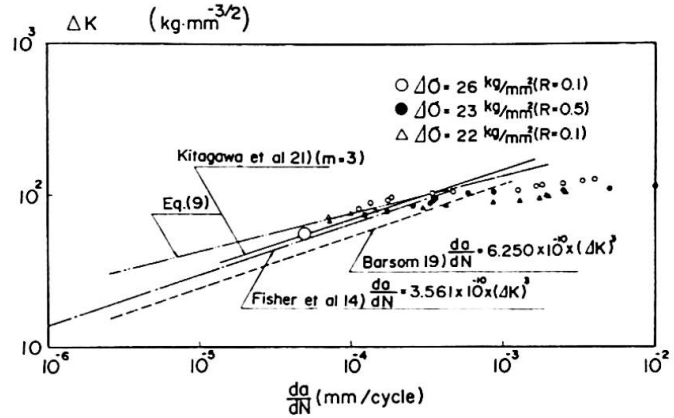
$$C = A / B^m \qquad\qquad\qquad \cdots\cdots\cdots\cdots\cdots \quad (10)$$

where A and B are constants for some range of materials ; $A = 0.5 \times 10^{-4}$, $B = 55$ for steels and $A = 10^{-4}$, $B = 55$ for aluminium alloys. The crack-growth relationship derived from eq. (10) in case of $m = 3$ is also shown in Fig. 10. It seems that the correlation given by eq. (10) is compared well with the one by Fisher et al. and predicts the conservative relation for the present test results. Despite the lack of data in the slower crack-growth rate region, these predictions give similar relations.

References

1) R. W. Frost and C. G. Schilling, ASCE, Proc., Vol. 90, No. ST3, June, 1964
2) H. S. Lew and A. A. Toprac, S. F. R. L. Tech. Rpt., p550—11, Janu., 1968
3) P. S. Carskaddan, Tech. Rpt. 57, 019-904(4), Applied Research Lab. U. S. Steel Corp.
4) R. W. Frost, Tech. Rpt., 57, 19-904(1), Applied Res. Lab., U. S. Steel Corp., Nov. 4, 1963
5) A. A. Toprac, Weld. J., May, 1969, 195-s 202-s
6) A. A. Toprac and M. Natarajan, ASCE, Proc., Vol. 97, No. ST4, 1971
7) Y. Maeda and Y. Kawai, 18th Conf. of Bridge and St. Eng. in Japan, p137
8) F. Nishino, M. Ito, M. Hoshino, JSSC, Vol. 7, No. 71, 1971 (in Japanese)
9) Y. Maeda, M. Ishiwata, Y. Kawai, IIW, Doc. XIII-734-74, April, 1974
10) Specs. for Highway Bridges, AASHTO, 1973
11) AISC Spec., Section 1.10, 1969, AISC
12) T. R. Gurney, Brit. Weld. J., July, 1962, p446
13) H. S. Reemsnyder, Weld. J., Oct., 1965, 458-s 465-s
14) M. A. Hirt, J. W. Fisher, Eng. Frac. Mech., 1973, Vol. 5, p415-429
15) J. W. Fisher, K. H. Frank, M. A. Hirt and B. M. Mcnamee, N. C. H. R. P., Rpt. No. 102, 1970
16) Y. Kikuchi and K. Yamada, JWS, Proc., Vol. 41, No. 9, 1972, p1085-1093
17) Interm Specs., Bridges, AASHTO., 1974
18) J. M. Barsom, U. S. Steel Corp., Applied Res. Lab., 1971
19) T. R. Gurney, Metal Const. and Brit. Weld. J., Feb., 1969, p91-96
20) H. Kitagawa et al., JSME, J, Vol. 75, 1972, p1068
21) P. C. Paris and F. Erdogan, ASME Trans., Vol. 85, Series D, No. 4, 1963

SUMMARY

   The data of fatigue strength of Type 3 crack in hybrid girders which initiate at tension flanges were explored and fatigue crack propagation behaviour at tension flanges and webs was studied by fracture mechanics analysis.

RESUME

   Les données de la résistance à la fatigue du Type 3 crack dans les poutres hybrides commençant par des brides de tension ont été explorées et le comportement propagateur de craquelage par fatigue aux brides de tension et âmes a été étudié par l'analyse mécanique de fracture.

ZUSAMMENFASSUNG

   Die Daten über Dauerfestigkeit des Anrisses vom Typ 3 an Hybridbalken, welche am Zuggurt beginnen, werden erörtert und das Ausbreitungsverhalten der Ermüdungsrisse an Zuggurten und Stegen werden mittels der Bruchmechanikanalyse untersucht.